CrossMark

Trajectory tracking control of an underactuated capsubot

M. Nazmul Huda[1,2] · Hongnian Yu[1]

Abstract Trajectory tracking control of underactuated systems is one of the challenging issues. This paper proposes a two-stage control strategy for the trajectory tracking of a class of underactuated mechanical systems. Two new acceleration profiles for the capsubot motion generation are proposed for the motion control of the capsubot. The optimum selection of the parameters of the acceleration profile is investigated. To track the trajectory of the capsubot, a selection algorithm is proposed. Simulation and experimentation are performed to demonstrate the feasibility of the control strategy and selection algorithm along with the newly proposed acceleration profiles.

Keywords Underactuated system · Capsubot · Two-stage control strategy · Selection algorithm

1 Introduction

A capsubot (capsule robot) is a robot which is limbless (i.e. no external moving parts) and moves using internal reaction force (Yu et al. 2008). A miniature capsubot might be suitable for in-vivo applications whereas a micro/miniature legged robot (Valdastri et al. 2009) may injure the internal

---

✉ Hongnian Yu
yuh@bournemouth.ac.uk

M. Nazmul Huda
nazmul.huda@coventry.ac.uk; nhuda@bournemouth.ac.uk;
m.n.huda@hotmail.com

[1] Bournemouth University, Bournemouth, UK

[2] Coventry University, Coventry, UK

soft tissues by the sharp edges of the legs. The capsubot might also be suitable for engineering diagnosis specially underground pipe inspection as the outer structure of the capsubot can be designed to match the desired pipe structure. Recently the research of micro/miniature robots, e.g. legged (Valdastri et al. 2009), earthworm-like (Menciassi et al. 2006) and capsule robots (Carpi et al. 2011; Carta et al. 2011; Zhang et al. 2011) have attracted the attention of researchers because of their potential applications such as medical diagnosis (e.g. capsule endoscopy) & treatments (e.g. drug delivery) and engineering diagnosis (e.g. underground pipe inspection) etc.

The capsubot is an underactuated system. The examples of underactuated systems are flexible link robots, legged robot with passive joints, cart-pole inverted pendulum (Park and Chwa 2009) or pendulum driven cart-pole system (Yu et al. 2008) or pendulum on a cart, inertia wheel pendulum (Lopez-Martnez et al. 2010), wheeled inverted pendulum (Pathak et al. 2005), helicopters, satellites, underwater vehicles etc.

Control of underactuated systems can be divided into two classes stabilization (Pathak et al. 2005; Huang et al. 2013; Xu and Özgüner 2008) and trajectory tracking control (Do et al. 2003; Aguiar and Hespanha 2007; Bi et al. 2010; Ashrafiuon et al. 2008). Two controllers (wheel velocity controller and vehicle position stabilization controller) were presented in Pathak et al. (2005) for a wheeled inverted pendulum (wheel movement active and pendulum movement passive) by utilizing partial feedback linearization. Three methods (feedback linearisation, Lyapunov design and sliding mode control) were combined in Lopez-Martnez et al. (2010) to achieve stabilization for a class of underactuated systems such as a pendulum on a cart where the pendulum movement is active and the wheel movement is passive. Sliding mode controller was designed in Huang et al. (2013) for an inverted pendulum based vehicle to control speed while stabilizing the body upright.

The Lyapunovs direct method and backstepping technique were used in Do et al. (2003) to develop a non-linear output-feedback controller for trajectory tracking of an underactuated vertical take-off and landing aircraft. Trajectory tracking of under-actuated vehicles such as hovercraft and under-water vehicle was addressed in Aguiar and Hespanha (2007) by combining adaptive switching supervisory control and Lyapunov based control. Trajectory tracking control of underactuated autonomous underwater vehicles is presented in Bi et al. (2010) based on Lyapunov stability theory by considering unknown ocean currents. A sliding mode control was used in Ashrafiuon et al. (2008) for trajectory tracking of underactuated surface vessels.

However trajectory tracking control of a class of underactuated systems utilizing the internal reaction force—such as pendulum on a cart (Lopez-Martinez et al. 2010) and a capsubot (Yu et al. 2011)—was not considered in the literature. In this paper trajectory tracking control of a capsubot is investigated. The capsubot is an underactuated system as it has one degree of freedom for the inner mass (IM) and one degree of freedom for the capsubot but the only control input is the force on the IM i.e. the movement of the IM is active whereas the movement of the capsubot is passive.

The capsubot driven by the internal reaction force has no external legs or wheels (Yu et al. 2008; Liu et al. 2008). The structure of the principle is derived from Yamagata and Higuchi (1995) where impact force and dry friction is utilised to create motion. A mass attached to the main object through a piezoelectric element, is made to move away from the main object rapidly and then to return to the initial position slowly with a sudden stop. The main object moves during the rapid motion and at the stopping moment and remains stationary for the rest of the time. The object can move along a straight line by repeating the above process. In Chernous'ko (2002) the propulsion principle was analyzed from the viewpoint of physics and a control law and optimum parameters of the system were proposed. In Lee et al. (2008), the motion generation of a single mass capsubot was explained on the basis of a four step velocity profile which is, fast motion for the first two steps and slow motion in the last two steps. In Liu et al. (2008), the motion generation of the capsubot was explained on the basis of a seven step velocity profile which is, fast motion in the first three steps and slow motion in the rest of the steps. A pendulum-driven cart was analysed in Yu et al. (2008) with a six step velocity profile. In Yu et al. (2011), motion of a single mass capsubot was explained on the basis of a novel four step acceleration profile.

However trajectory tracking control of the capsubot was not considered in all the above mentioned researches though it is the primary requirement of a mobile robot. Trajectory tracking control for this type of underactuated mechanical systems is still an open issue. This research presents a strategy to solve this issue.

Main contributions of the paper are (a) proposed a new two-stage control strategy for the trajectory tracking control of a capsubot; (b) modified the acceleration profile of Yu et al. (2011) and proposed two new acceleration profiles (utroque and contrarium) for the capsubot motion generation; (c) implemented the acceleration profiles in a developed self-contained capsubot; (d) proposed a novel selection algorithm for the proper selection of the acceleration profile (i.e utroque or contrarium) and also to select the correct acceleration profile parameters (acceleration values) (e) implemented the proposed trajectory tracking control strategy in the developed capsubot.

The paper is structured as below. Section 2 presents the modelling of the capsubot, explains the problem and proposes a control strategy for trajectory tracking for a class of underactuated system. Section 3 proposes two new acceleration profiles modified from Yu et al. (2011) and explains the motion generation of the capsubot for both the acceleration profiles. The motivation to propose the acceleration profiles are also explained and discussed in Sect. 3. The control approach is explained in detail in Sect. 4. Simulation and experimentation results are presented in Sect. 5 to demonstrate the feasibility of the proposed control strategy. Finally the conclusions and some future works are given in Sect. 6.

2 Modelling, problem statement and proposed strategy

2.1 Dynamic modelling

Figure 1 shows a schematic of the studied capsubot. The inner mass (IM) can move from one end to the other end of the capsubot. The source of the propulsion force is not shown here. By controlling the IM, the capsubot can be moved in a certain given direction. The dynamic model of the capsubot is:

$$F_m = m\ddot{x}_m + f_m \tag{1}$$
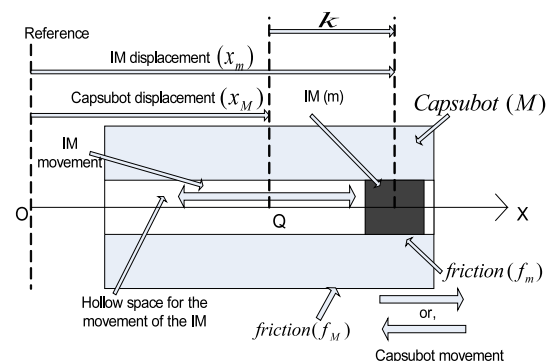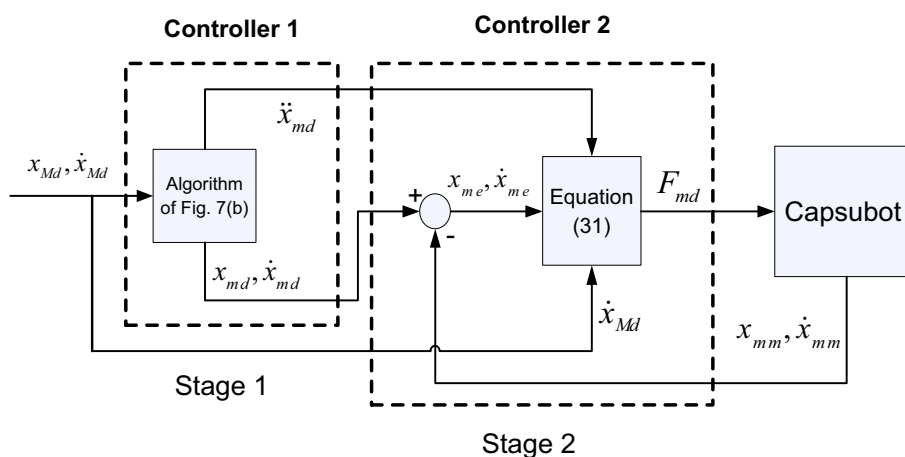$$F_M = -(Fm - fm) = (M - m)\ddot{X}_m + f_M \tag{2}$$

Fig. 1 Schematic of the capsubot (conceptual)

Fig. 2 Schematic diagram of the proposed control system of the capsubot

where M is capsubot mass and m is IM mass; x_m and x_M are the positions of the IM and the capsubot with respect to an external reference; F_m is the force on the IM; F_M is the force received by the capsubot due to IM movement; $f_M = sgn(\dot{x}_M)\mu_M Mg$ and $f_m = sgn(\dot{x}_m - \dot{x}_M)\mu_m mg$ are the friction between the capsubot and the surface of motion, and between the IM and the capsubot respectively. Here μ is the coulomb friction coefficient. The initial position of the mid-point of the capsubot is taken as the reference for the measurement of x_m and x_M.

2.2 Problem statement and proposed strategy

Trajectory tracking control of the capsubot is still an open issue due to that it is an underactuated system in nature. To solve this problem we divide the control problem into two stages which are described below. The schematic diagram of the complete control system is shown in Fig. 2.

– Stage 1 *Desired IM Trajectory Generation*: For a given trajectory $(x_{Md}, \dot{x}_{Md})$ of the capsubot, the desired trajectory $(x_{md}, \dot{x}_{md}, \ddot{x}_{md})$ of the IM is calculated.
– Stage 2 *Control of the IM*: For the given desired trajectory $(x_{md}, \dot{x}_{md}, \ddot{x}_{md})$ of the IM, the closed-loop control is achieved by correcting the control input using the error $(x_{me}, \dot{x}_{me}, \ddot{x}_{me})$ which is the difference between the measured and the desired trajectories of the IM.

These two stages are followed in the remaining paper.

3 Proposed acceleration profiles and motion generation

3.1 Proposed acceleration profiles

In this paper trajectory tracking of a capsubot is performed using a two-stage control approach (see Fig. 2). To do that the capsubot trajectory is divided into small pieces. The IM

acceleration profile parameters are tuned in every piece to enable the capsubot to track the trajectory. In Yu et al. (2011), a 4-step acceleration profile of IM is proposed for the motion generation of a capsubot. We faced the following issues while trying to follow the capsubot trajectory using the acceleration profile of Yu et al. (2011).

– For a set of parameters (accelerations) of IM, the cycle time is different for cycle 1 and the other cycles.
– From cycle 2, the capsubot has a nonzero initial velocity which depends upon the previous cycle. Thus the distance travelled by the capsubot in each cycle not only depends on the IM accelerations of that particular cycle but also on the previous cycle.

Based on these observations acceleration profile of Yu et al. (2011) is modified and following two acceleration profiles: utroque and contrarium are proposed where (a) cycle times are same for all the cycles for a specific parameter (acceleration) set and (b) the capsubot has a zero initial velocity in all the cycles. Here the distance travelled by the capsubot in each cycle solely depends on the IM accelerations of that cycle. This makes the trajectory following problem easier to solve. Utroque is a four-step acceleration profile whereas contrarium is a two-step acceleration profile. It is worth mentioning that steps 3 and 4 of the utroque profile are similar to steps 1 and 2 of the contrarium profile respectively apart from a nonzero capsubot initial velocity in step 3 of the utroque profile.

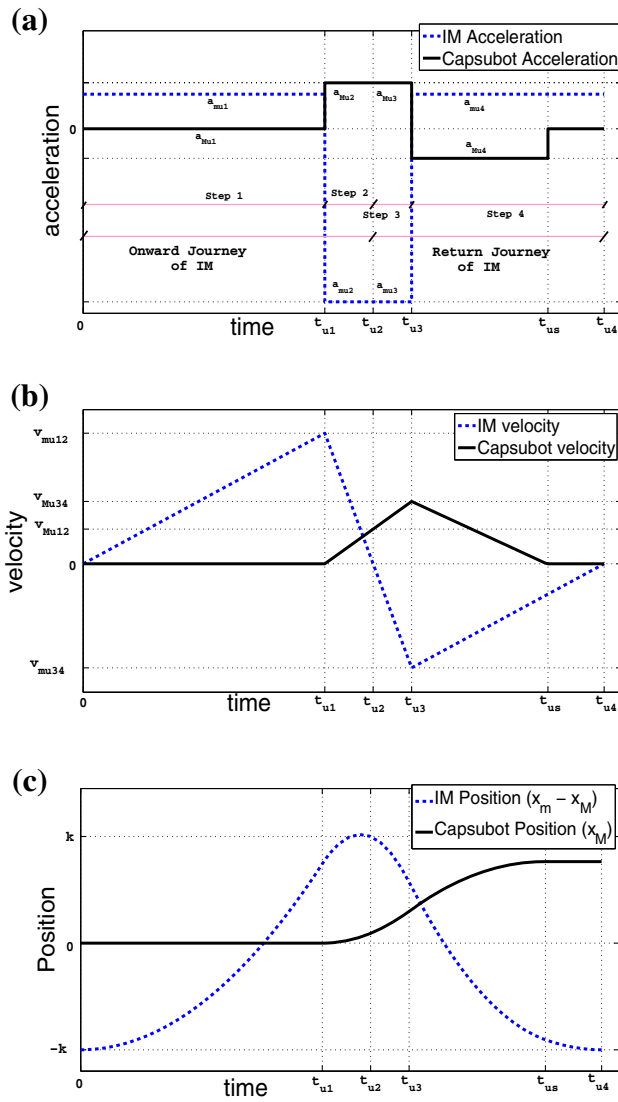### 3.1.1 Utroque acceleration profile

This is a four-step acceleration profile shown in Fig. 3a, b. The scenarios of the capsubot movement in this profile are shown in Fig. 4a, b. In this profile, the capsubot and the IM move in the same direction in step 2 (see Fig. 5b) and moves in the opposite direction in steps 3 and 4. The IM moves forward (onward journey) for steps 1 and 2, and backward (return
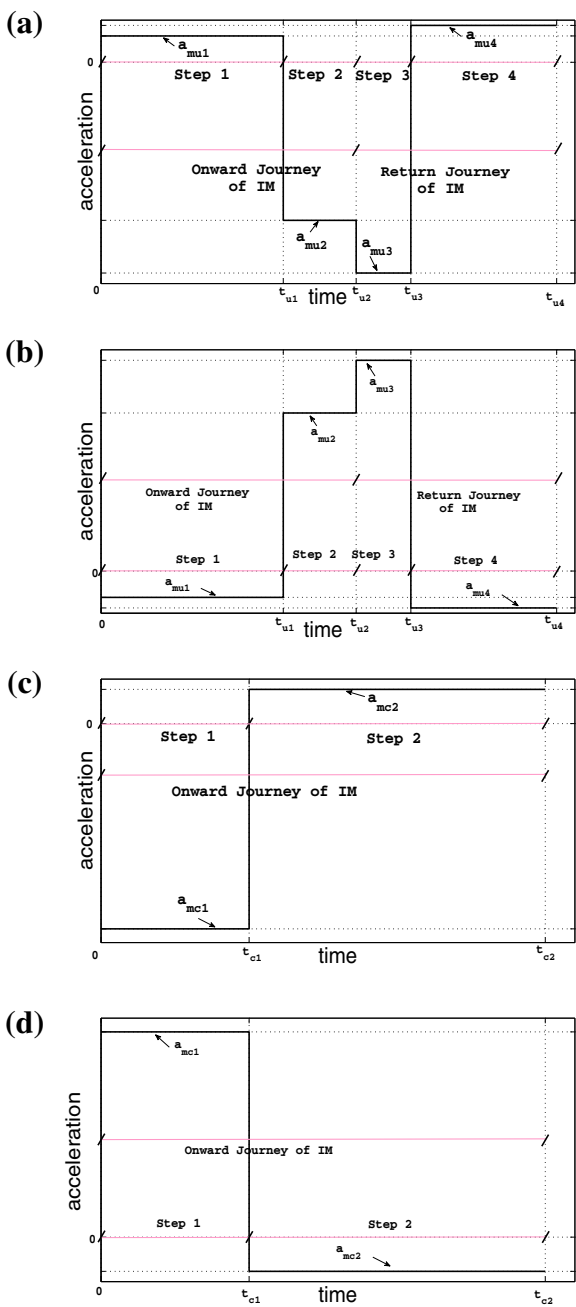
Fig. 3 Acceleration profiles for IM. **a** Utroque acceleration profile—Scenario 1 (a_{mu1}, a_{mu2}, a_{mu3} and a_{mu4} are the IM accelerations in steps 1, 2, 3 and 4 respectively; t_{u1}, t_{u2}, t_{u3} and t_{u4} are the time after steps 1, 2, 3 and 4 respectively). **b** Utroque acceleration profile—Scenario 2 (a_{mu1}, a_{mu2}, a_{mu3} and a_{mu4} are the IM accelerations in steps 1, 2, 3 and 4 respectively; t_{u1}, t_{u2}, t_{u3} and t_{u4} are the time after steps 1, 2, 3 and 4 respectively). **c** Contrarium acceleration profile—Scenario 1 (a_{mc1} and a_{mc2} are the IM accelerations in steps 1 and 2 respectively; t_{u1} and t_{u2} are the time after steps 1 and 2 respectively). **d** Contrarium acceleration profile—Scenario 2 (a_{mc1} and a_{mc2} are the IM accelerations in steps 1 and 2 respectively; t_{u1} and t_{u2} are the time after steps 1 and 2 respectively)
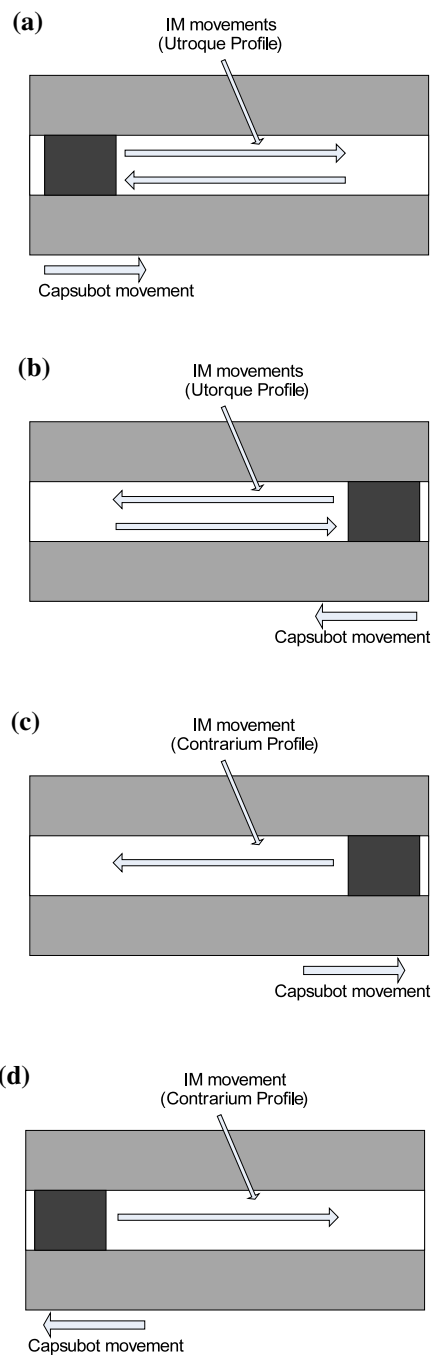
Fig. 4 Four possible scenarios for the capsubot motion. **a** For the IM at the *left end*, the capsubot is moved to the *right* using the Utroque profile shown in Fig. 3a. **b** For the IM at the *right end*, the capsubot is moved to the *left* using the Utroque profile shown in Fig. 3b. **c** For the IM at the *right end*, the capsubot is moved to the *right* using the Contrarium profile of Fig. 3c. After one cycle the IM reaches to the *left end* and then the IM uses the Utroque profile described in Fig. 4a. **d** For the IM at the *left end*, the capsubot is moved to the *left* using the Contrarium profile of Fig. 3d. After one cycle the IM reaches to the *right end* and then the IM uses the Utroque profile described in Fig. 4b
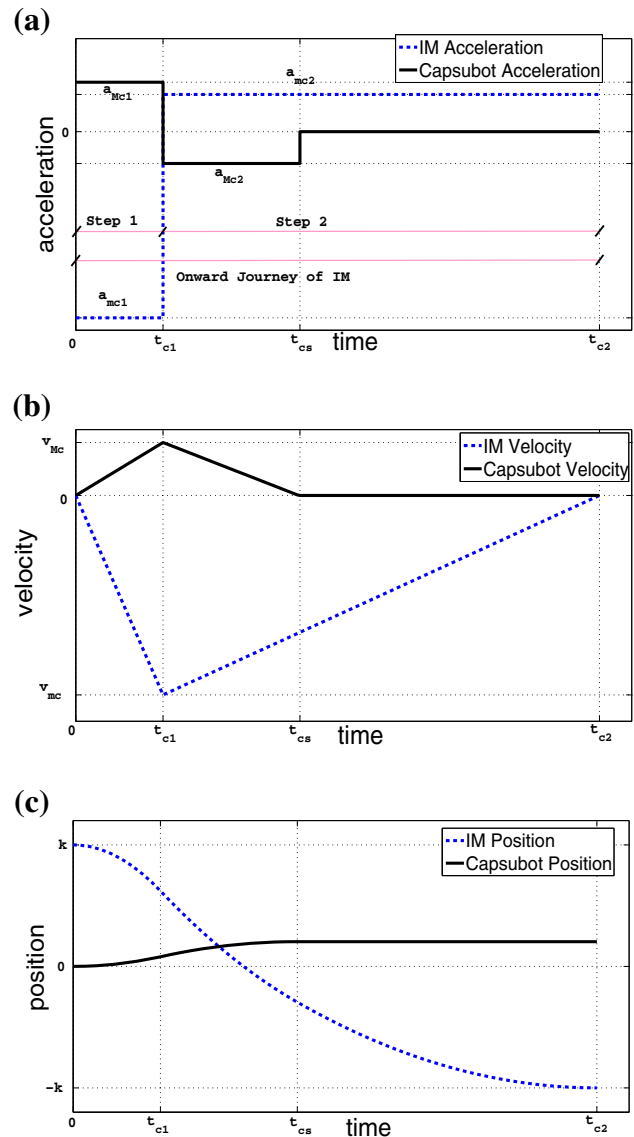
Fig. 5 Accelerations, velocities and positions of the IM and the capsubot for Utroque profile for the scenario of Figs. 4a and 3a. **a** IM and capsubot accelerations. **b** IM and capsubot velocities. **c** IM and capsubot positions

journey) for steps 3 and 4. The capsubot moves forward for steps 2, 3 and 4. Thus the capsubot moves forward for IM bidirectional movements. Latin word 'utroque' means both directions. a_{mu1} and a_{mu4} can be taken same or different. Similarly a_{mu2} and a_{mu3} can be taken same or different.

3.1.2 Contrarium acceleration profile

This is a two-step acceleration profile shown in Fig. 3c, d. The scenarios of the capsubot movement in this profile are shown in Fig. 4c, d. In this profile, the capsubot moves in the opposite direction of the IM (see Fig. 6b). Latin word 'contrarium' means the opposite direction. Here the IM only performs onward journey.

Fig. 6 Accelerations, velocities and positions of the IM and the capsubot for Contrarium profile for the scenario of Figs. 4c and 3c. **a** IM and capsubot accelerations. **b** IM and capsubot velocities. **c** IM and capsubot positions

3.2 Motion generation

Four possible scenarios are shown in Fig. 4a-d. Motion generation is explained for two scenarios (Fig. 4a, c) based on the two proposed acceleration profiles. Motion generation of the scenarios of Fig. 4b, d are similar in principle to the scenarios of Fig. 4a, c respectively.

3.2.1 Utroque acceleration profile for the scenario of Fig. 4a

The IM is at its left end ($x_m - x_M = -k$) at the beginning of the cycle and the IM follows the acceleration profile shown

in Fig. 3a. Here k is the half length of maximum relative displacement of the IM. The IM moves from the left end to the right end and then returns to the left end in this acceleration profile. Accelerations, velocities and positions of the IM and the capsubot in different steps are shown in Fig. 5a–c and $a_{mu1} = a_{mu4}$ and $a_{mu2} = a_{mu3}$.

Step 1 The IM moves forward slowly with a small +ve acceleration ($a_{mu1} > 0$, $\dot{x}_m > 0$) and, as the friction force (f_M) dominates over the reaction force (F_M) i.e. $|F_M| < |f_M|$, the capsubot remains standstill ($\ddot{x}_M = 0$, $\dot{x}_M = 0$).

Step 2 The IM moves forward with a big -ve acceleration ($a_{mu2} << 0$, $\dot{x}_m > 0$) and the capsubot moves forward with a +ve acceleration ($a_{Mu2} > 0$, $\dot{x}_M > 0$) due to the reaction force (F_M) where $|F_M| > |f_M|$. The IM reaches to its right end ($x_m - x_M = k$) at the end of this step and stops.

Step 3 In this step the capsubot has a +ve initial velocity ($v_{Mu12} > 0$). The IM moves backward with a big -ve acceleration ($a_{mu3} << 0$, $\dot{x}_m < 0$) and the capsubot receives a force (F_M) in the forward direction where $|F_M| > |f_M|$. Thus the capsubot moves forward with a +ve acceleration ($a_{Mu3} > 0$, $\dot{x}_M > 0$). The capsubot velocity in this step is higher than in step 2.

Step 4 The IM continues to move backward but with a small +ve acceleration ($a_{mu4} > 0$, $\dot{x}_m < 0$). The capsubot moves forward with a small -ve acceleration ($a_{Mu4} < 0$, $\dot{x}_M > 0$) for a part of step 4 before it stops. The capsubot remains standstill ($\ddot{x}_M = 0$, $\dot{x}_M = 0$) for the remaining time of step 4 as the friction force (f_M) dominates over the reaction force (F_M) i.e. $|F_M| < |f_M|$. The IM reaches to its left end ($x_m - x_M = -k$) at the end of step 4 and stops.

In Fig. 5a–c we see that, in steps 1 and 2 the IM completes the onward journey and reaches to k position from $-k$ postion. In step 1 the IM has a small +ve acceleration ($a_{mu1} > 0$) and thus the IM slowly reaches to v_{mu12} velocity from zero velocity whereas the capsubot remains standstill for the entire step 1 and, the capsubot velocity and acceleration are zero. In step 2 the IM has a big -ve acceleration ($a_{mu2} << 0$) and thus the IM velocity reaches to zero from v_{mu12} in a shorter period of time and also the IM travels shorter distance in step 2 comparing to step 1. The capsubot moves forward with a moderate acceleration (a_{Mu2}) and it reaches to v_{Mu12} velocity from zero in step 2.

In steps 3 and 4 the IM completes its return journey and returns to $-k$ position from k position. In step 3 the IM moves with a big -ve acceleration and at a shorter time period IM velocity reaches to v_{mu34} from zero. The capsubot keeps moving forward with a moderate acceleration (a_{Mu3}) and the IM velocity reaches to v_{Mu34} from v_{Mu12} in step 3 where

$v_{Mu34} > v_{Mu12}$. As in step 3 the capsubot has a non-zero initial velocity, the capsubot average velocity in step 3 is bigger than that in step 2. We see from Fig. 5c that the distance travelled by the capsubot in step 3 is bigger than that in step 2. In step 4 the IM moves with a small +ve acceleration (a_{mu4}) and the IM velocity reaches to zero from v_{mu34}. The capsubot moves forward with a -ve acceleration (a_{Mu4}) and stops at t_{us} time. Thus the capsubot moves in steps 2, 3 and part of step 4 and remains stationary at the rest of the time.

3.2.2 Contrarium acceleration profile for the scenario of Fig. 4c

The IM is at its right end ($x_m - x_M = k$) at the beginning of the cycle and the IM follows the acceleration profile shown in Fig. 3c. The IM moves from right end to left end in this acceleration profile. Accelerations, velocities and positions of the IM and the capsubot in different steps are shown in Fig. 6a–c. This is a two-step acceleration profile.

Step 1 The IM moves backward with a big -ve acceleration ($a_{mc1} << 0$, $\dot{x}_m < 0$) and the capsubot receives a force ($F_M > 0$) in the forward direction. Here the reaction force (F_M) is big enough to overcome the friction (f_M) i.e. $|F_M| > |f_M|$. Thus the capsubot moves forward with a +ve acceleration ($a_{Mc1} > 0$, $\dot{x}_M > 0$).

Step 2 The IM continues to move backward but with a small +ve acceleration ($a_{mc2} > 0$, $\dot{x}_m < 0$). The capsubot moves forward with a small -ve acceleration ($a_{Mc2} < 0$, $\dot{x}_M > 0$) for a part of step 2 before it stops. The capsubot remains standstill ($\ddot{x}_M = 0$, $\dot{x}_M = 0$) for the remaining time of step 2 as the friction force (f_M) dominates over the reaction force (F_M) i.e. $|F_M| < |f_M|$. The IM reaches its left end ($x_m - x_M = -k$) at the end of step 2 and stops.

3.3 Optimum selection of acceleration profile parameters

The optimum values of a_{mc1}, a_{mc2}, a_{mu1}, a_{mu2}, a_{mu3}, a_{mu4}, t_{c1}, t_{c2}, t_{u1}, t_{u2}, t_{u3} and t_{u4} in Fig. 3a–d are selected to achieve the best performance. a_{mc1}, a_{mu2} and a_{mu3} are big accelerations and they can be taken as big as possible (depending on the maximum force the propulsion source can provide) to get a big average velocity of the capsubot. a_{mc2}, a_{mu1} and a_{mu4} should be small enough so that the friction force (f_M) is bigger than the reaction force (F_M), thus the capsubot does not move reverse. Thus using (1) and (2) we observe that $|a_{mc2}|$, $|a_{mu1}|$, $|a_{mu4}|$ are less than $\frac{\mu_M M g}{m}$. We may take $a_{mu1} = a_{mu4}$ and $a_{mu2} = a_{mu3}$ or, $a_{mu1} \neq a_{mu4}$ and $a_{mu2} \neq a_{mu3}$ or, $a_{mu1} = a_{mu4}$ and $a_{mu2} \neq a_{mu3}$ or, $a_{mu1} \neq a_{mu4}$ and $a_{mu2} = a_{mu3}$. Here we have designed $a_{mu1} = a_{mu4}$ and $a_{mu2} = a_{mu3}$.

Utroque profile From Fig. 5a, b, we have

$$t_{u1} = \frac{|v_{mu12}|}{|a_{mu1}|} \; ; \quad t_{u2} = t_{u1} + \frac{|v_{mu12}|}{|a_{mu2}|} \tag{3}$$

$$t_{u3} = t_{u2} + \frac{|v_{mu34}|}{|a_{mu3}|}; \quad t_{u4} = t_{u3} + \frac{|v_{mu34}|}{|a_{mu4}|} \tag{4}$$

$$t_{us} = t_{u3} + \frac{|v_{M34}|}{|a_{Mu4}|} \tag{5}$$

where,

$$v_{mu12} = \sqrt{\frac{4k a_{mu1} a_{mu2}^2}{a_{mu2}^2 - a_{mu1} a_{mu2} - a_{mu1} a_{Mu2}}} \tag{6}$$

$$a_{Mui} = \frac{-m a_{mui} - \mu_M M g}{M}; \quad i = 2, 3, 4 \tag{7}$$

$$v_{Mu12} = -\frac{a_{Mu2}}{a_{mu2}} v_{mu12} \tag{8}$$

$$v_{Mu34} = \frac{a_{Mu3}}{a_{mu3}} v_{mu34} + v_{Mu12} \tag{9}$$

and v_{mu34} can be found by solving the quadratic equation of v_{mu34} shown below:

$$\left(\frac{1}{a_{mu3}} - \frac{1}{a_{mu4}} + \left(\frac{1}{a_{Mu4}} - \frac{1}{a_{Mu3}} \right) \frac{a_{Mu3}^2}{a_{mu3}^2} \right) v_{mu34}^2$$

$$+ 2 v_{mu12} \frac{a_{Mu3} a_{Mu2}}{a_{mu3} a_{mu2}} \left(\frac{1}{a_{Mu4}} - \frac{1}{a_{Mu3}} \right) v_{mu34}$$

$$+ \left(4k + \frac{v_{Mu12}^2 a_{Mu2}^2}{a_{Mu4} a_{mu2}^2} v_{mu12}^2 \right) = 0 \tag{10}$$

Contrarium profile From Fig. 6a, b, we have

$$t_{c1} = \frac{|v_{mc}|}{|a_{mc1}|}; \quad t_{c2} = t_{c1} + \frac{|v_{mc}|}{|a_{mc2}|} \tag{11}$$

$$t_{cs} = t_{c1} + \frac{|v_{Mc}|}{|a_{Mc2}|} \tag{12}$$

where,

$$v_{Mc} = \frac{a_{Mc1}}{a_{mc1}} v_{mc} \tag{13}$$

$$v_{mc} = -\sqrt{\frac{-4k a_{mc1}^2 a_{mc2} a_{Mc2}}{a_{mc1} a_{Mc2} P - a_{Mc1} a_{mc2} Q}} \tag{14}$$

where $P = a_{mc2} - a_{mc1}$; $Q = a_{Mc2} - a_{Mc1}$ and a_{Mc1}, a_{Mc2} can be calculated as:

$$a_{Mci} = \frac{-m a_{mci} - \mu_M M g}{M}; \quad i = 1, 2 \tag{15}$$

It is noted that we can avoid that the denominators of (3)–(14) equal to zero since $a_{mc1}, a_{mc2}, a_{mu1}, a_{mu2}, a_{mu3}$, and a_{mu4} are selected by the designer.

3.4 Comparison with other profiles

Lee et al. (2008) and Liu et al. (2008) analysed the motion generation of capsubot type robot based on velocity profiles. Lee et al. (2008) proposed a four-step velocity profile whereas Liu et al. (2008) proposed a seven-step velocity profile. Through simulation and experimental results Yu et al. (2011) demonstrated the advantages of using acceleration profile over velocity profile to analyse and control the capsubot type robot motion. The acceleration profile of Yu et al. (2011) is modified in this paper and two new acceleration profiles are proposed.

To decide on the optimum number of steps to generate capsubot motion, previous works used various criteria. A new step is defined (i) in Liu et al. (2008) whenever there is a change of IM acceleration (ii) in Lee et al. (2008) whenever there is a change of capsubot acceleration or change of IM velocity direction (iii) in Yu et al. (2011) whenever there is a change of IM acceleration or change of IM velocity direction.

At least two steps are required by the IM to go from one end to the other end of the capsubot, as the IM needs to accelerate to start motion and then decelerate to stop. As in contrarium cycle the IM performs only onward journey i.e. it goes from one end to the other end, it needs at least two steps. On the other hand as in utroque profile the IM performs onward and return journeys i.e. it goes from one end to the other end and then returns to its original position, it needs at least four steps.

All the previous works define the profiles for a round trip of the IM (i.e. for onward and return journeys of IM). Thus all the proposed profiles used at least four steps: Lee et al. (2008); Yu et al. (2011) used four and Liu et al. (2008) used seven. An analysis is provided below whether adding extra three steps in Liu et al. (2008) provides any added advantage. Liu et al. (2008) used three steps for IM onward journey and four steps for IM return journey. On the onward journey: step 1 is large IM acceleration, step 2 is large deceleration, step 3 is small deceleration. However in the onward journey the only requirement is to keep the IM acceleration such that the capsubot only moves forward. To maintain that steps 2 and 3 can be merged to get one step. From the simulation result in Liu et al. (2008) we see that there is reverse motion of the capsubot presumably in step 2 because of large deceleration. Thus step 2 can be removed and we can keep only steps 1 and 3. On the return journey: step 4 is motionless step, step 5 is small acceleration, step 6 is constant velocity movement and step 7 is small deceleration to stop. However in the return journey the only requirement is to maintain the IM acceleration such that the capsubot does not have any reverse motion. That can be fulfilled only by two steps.

4 Proposed control approach

The objective is to follow a given trajectory (position, x_{Md}) of the capsubot. The objective is achieved using the two-stage approach of Fig. 2. The following steps are followed:

– Stage 1 Desired IM Trajectory Generation (Sect. 4.1)

– Step 1 Generating capsubot trajectory piece and selection of Piece Period (T) (Sect. 4.1.1)
– Step 2 Data-base creation (Sect. 4.1.2)
– Step 3 Selection of Profile Parameters (Selection Algorithm) (Sect. 4.1.3)
– Step 4 Tuning the Piece Time (Sect. 4.1.4)

– Stage 2 Control of the IM (Sect. 4.2)

4.1 Stage 1: Desired IM trajectory generation

The control requirement is to make the capsubot follow a given trajectory. As the capsubot is an underactuated system, the movements of the capsubot cannot be controlled directly (i.e. x_M is uncontrollable directly). The capsubot movements are controlled indirectly by controlling the movements of the IM (x_m is controllable directly). The capsubot average velocity can be tuned by changing the parameters of the IM acceleration profile ($\bar{\ddot{x}}_M = f(x_m, \ddot{x}_m)$). Let the capsubot follow the position trajectory shown in Fig. 7a. The desired capsubot velocity changes throughout the trajectory. Thus to track the trajectory we need to change the IM acceleration profile parameters so that the capsubot average velocity changes according to the desired value. To track the capsubot trajectory primarily the utroque profile is used. The contrarium profile is used for one cycle when capsubot velocity changes from negative to positive or positive to negative. Then the IM continues to follow the utroque profile. In the desired trajectory for path A–B the capsubot velocity is positive and for path B–C the capsubot velocity is negative. Thus the IM follows the utroque profile of Fig. 3a for A–B path (but changes the parameters to tune the capsubot average velocity to track the trajectory) and then uses the contrarium profile of Fig. 3d for one cycle and then follows the utroque profile of Fig. 3b for B–C path (but changes the parameters to tune the capsubot average velocity to track the trajectory).

4.1.1 Step 1: Generating capsubot trajectory piece and selection of piece period (T)

Pieces (shown in Fig. 7a) are designed based on the desired trajectory. T is the time duration of each piece. $\delta x_M(i)$ is the required displacement in the ith piece. Now desired average velocity in the ith piece is:
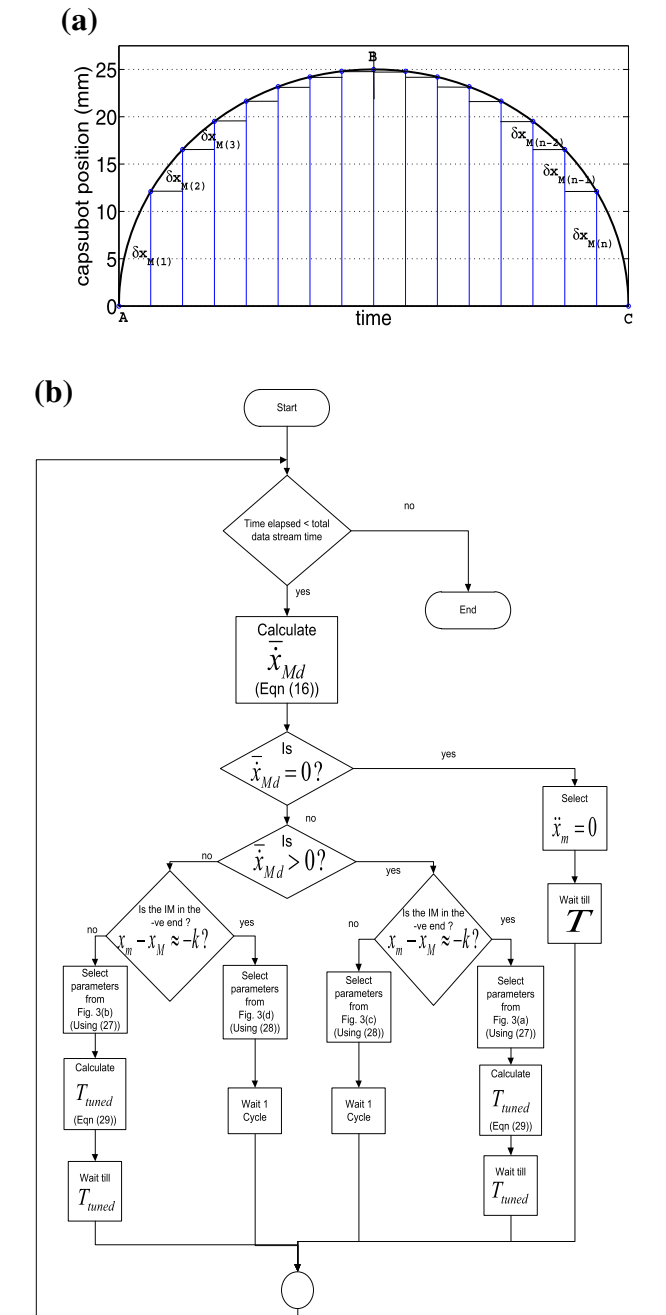
Fig. 7 Desired trajectory and selection algorithm. **a** Desired trajectory of the capsubot (Piece-wise tracking). **b** Flow chart of the selection algorithm

$$\bar{\dot{x}}_{Md}(i) = \frac{\delta x_M(i)}{T} \tag{16}$$

A smaller T provides smoother tracking of trajectory. But T cannot be infinitesimally small as the IM has to complete at least one cycle with one acceleration profile with one set of parameters once it starts, before it can start another cycle with different acceleration profile parameters. Thus the minimum piece period is:

$$T_{min} = max\big(max(t_c), max(t_u)\big) \tag{17}$$

where, t_c and t_u are the cycle time of contrarium profile and utroque profile respectively.

4.1.2 Step 2: Data-base creation

To track the capsubot trajectory we need to know the projected capsubot average velocities for various IM acceleration profile parameters. Equations for projected average velocities are given below. The capsubot average velocity for the utroque profile is (see Fig. 5c):

$$\bar{\dot{x}}_{Mu} = \frac{x_{Mu}}{t_u} \tag{18}$$

where x_{Mu} is the displacement of the capsubot in utroque profile in cycle time t_u.

$$x_{Mu} = \frac{v_{Mu12}^2}{2a_{Mu2}} + \frac{v_{Mu34}^2 - v_{Mu12}^2}{2a_{Mu3}} - \frac{v_{Mu34}^2}{2a_{Mu4}} \tag{19}$$

$$t_u = t_{u4} = \frac{|v_{mu12}|}{|a_{mu1}|} + \frac{|v_{mu12}|}{|a_{mu2}|} + \frac{|v_{mu34}|}{|a_{mu3}|} + \frac{|v_{mu34}|}{|a_{mu4}|} \tag{20}$$

The average velocity of the capsubot for the contrarium profile is (see Fig. 6c):

$$\bar{\dot{x}}_{Mc} = \frac{x_{Mc}}{t_c} \tag{21}$$

where x_{Mc} is the displacement of the capsubot in contrarium profile in cycle time t_c.

$$x_{Mc} = \frac{v_{Mc}^2}{2a_{Mc1}} - \frac{v_{Mc}^2}{2a_{Mc2}} \tag{22}$$

$$t_c = t_{c2} = \frac{|v_{mc}|}{|a_{mc1}|} + \frac{|v_{mc}|}{|a_{mc2}|} \tag{23}$$

For the utroque profile we can change four parameters namely a_{mu1}, a_{mu2}, a_{mu3} and a_{mu4} to get different capsubot average velocities. In this paper, we use $a_{mu2} = a_{mu3}$ and $a_{mu1} = a_{mu4}$. We also choose a fixed value for $a_{mu1} = a_{mu4}$ (maintaining $|a_{mu1}| = |a_{mu4}| < \frac{\mu_M M g}{m}$). We tune only $a_{mu2} = a_{mu3}$ to get different capsubot average velocities. If a_{mumax} is the maximum possible acceleration, a_{mumin} is the minimum and a_{mudiff} is the difference between two consecutive profile parameter sets, then total number of acceleration profile sets for the utroque profile is:

$$n_u = \frac{a_{mumax} - a_{mumin}}{a_{mudiff}} + 1 \tag{24}$$

For the contrarium profile we can change two parameters namely a_{mc1} and a_{mc2} to get different capsubot average velocities. We choose a fixed value for a_{mc2} (maintaining

$|a_{mc2}| < \frac{\mu_M M g}{m}$). We tune only a_{mc1} to get different capsubot average velocities. If a_{mcmax} is the maximum acceleration, a_{mcmin} is the minimum and a_{mcdiff} is the difference between two consecutive profile parameter sets, then total number of profile parameter sets for the contrarium profile is:

$$n_c = \frac{a_{mcmax} - a_{mcmin}}{a_{mcdiff}} + 1 \tag{25}$$

The maximum capsubot average velocity will be:

$$\bar{\dot{x}}_{Mmax} = max\big(max(\bar{\dot{x}}_{Mc}), max(\bar{\dot{x}}_{Mu})\big) \tag{26}$$

where

$$max(\bar{\dot{x}}_{Mc}) = max\big((\bar{\dot{x}}_{Mc})_1, (\bar{\dot{x}}_{Mc})_2, \ldots (\bar{\dot{x}}_{Mc})_{n_c}\big)$$
$$max(\bar{\dot{x}}_{Mu}) = max\big((\bar{\dot{x}}_{Mu})_1, (\bar{\dot{x}}_{Mu})_2, \ldots (\bar{\dot{x}}_{Mu})_{n_u}\big)$$

Average velocities of the capsubot for different profile parameters for two acceleration profiles are calculated and stored in the database.

4.1.3 Step 3: Selection of profile parameters (selection algorithm)

$\bar{\dot{x}}_{Md}$ is compared with the database created in Sect. 4.1.2 for each piece of the capsubot trajectory. Following two steps are followed:

1. One profile is selected from the four profiles described in Fig. 3. Normally one of the two utroque acceleration profiles is used: profile of Fig. 3a for positive $\bar{\dot{x}}_{Md}$ and profile of Fig. 3b for negative $\bar{\dot{x}}_{Md}$. In the utroque acceleration profile the IM returns to its initial position at the end of each cycle. Thus one of the two contrarium acceleration profiles (Fig. 3c or d) is used whenever a switching between the two utroque acceleration profiles is required.

2. For utroque profile we need to select the profile parameters: a_{mu1}, a_{mu2}, a_{mu3} and a_{mu4} which will generate the required desired average velocity ($\bar{\dot{x}}_{Md}$). From the database created, we get $\bar{\dot{x}}_{Mu}(p)$, $p = 1, 2, \ldots, n_u$ i.e. all the possible profile parameters and corresponding projected average velocities. The desired average velocity ($\bar{\dot{x}}_{Md}$) is compared with projected average velocities as shown in (27). The profile parameter-set corresponding to minimum error of (27) is selected.

$$\dot{x}_{diff} = min\Big((|\bar{\dot{x}}_{Md}| - |\bar{\dot{x}}_{Mu}(1)|),$$
$$(|\bar{\dot{x}}_{Md}| - |\bar{\dot{x}}_{Mu}(2)|), \ldots, (|\bar{\dot{x}}_{Md}| - |\bar{\dot{x}}_{Mu}(n_u)|)\Big) \tag{27}$$

For the contrarium cycle we need to select the profile parameters: a_{mc1} and a_{mc2} which will generate the

required desired average velocity ($\bar{\dot{x}}_{Md}$). From the database created, we get $\bar{\dot{x}}_{Mc}(p)$, $p = 1, 2, \ldots, n_c$ i.e. all the possible profile parameters and corresponding projected average velocities. The desired average velocity ($\bar{\dot{x}}_{Md}$) is compared with projected average velocities as shown in (28). The profile parameter-set corresponding to minimum error of (28) is selected.

$$\dot{x}_{diff} = min\Big(\big(|\bar{\dot{x}}_{Md}| - |\bar{\dot{x}}_{Mc}(1)|\big),$$
$$\big(|\bar{\dot{x}}_{Md}| - |\bar{\dot{x}}_{Mc}(2)|\big), \ldots, \big(|\bar{\dot{x}}_{Md}| - |\bar{\dot{x}}_{Mc}(n_c)|\big)\Big) \quad (28)$$

The piece is taken from the desired trajectory with a piece period considering the constraint (17). In each piece the IM is required to follow a specific acceleration profile with a specific profile parameter set to track the desired trajectory. We propose a selection algorithm to select the right acceleration profile with right profile parameters in each piece. The selection algorithm is presented in Fig. 7b. Selection algorithm incorporates all the logical development presented in Sect. 4.1.3. It also uses database created in Sect. 4.1.2 and, equations developed in Sects. 4.1.1 and 4.1.4.

4.1.4 Step 4: Tuning the piece time

An acceleration profile with a profile parameter set cannot be operated for any discrete amount of time but for a multiple of the cycle time of that acceleration profile with that parameter set. The selected parameter set will be used for the following time span:

$$T_{tuned} = t_{sel} \times floor\left(\frac{T}{t_{sel}}\right) \quad (29)$$

where t_{sel} is the cycle time of the selected utroque profile; floor(A) rounds the elements of A to the nearest integers less than or equal to A.

4.2 Stage 2: Control of the IM

Open loop control law of the IM is:

$$F_{md} = m\ddot{x}_{md} + sgn(\dot{x}_{md} - \dot{x}_{Md})\mu_m mg \quad (30)$$

The closed-loop control law can be selected, using partial feedback linearization (Yu et al. 2008):

$$F_{md} = \alpha\tau_{md} + \beta \quad (31)$$

where $\alpha = m$ and $\beta = sgn(\dot{x}_{md} - \dot{x}_{Md})\mu_m mg$

Let $\tilde{x}_m = x_{me} = x_{mm} - x_{md}$ be the tracking error; choosing the linear control law $\tau_{md} = \ddot{x}_m - k_1\dot{\tilde{x}}_m - k_2\tilde{x}_m$ and

Table 1 Parameters of the developed capsubot

M	m	μ_M	μ_m	k
$0.396kg$	$0.05kg$	0.1	0.2	$9mm$

applying the control law of (31) to (1) we get the error equation,

$$\ddot{\tilde{x}}_m + k_1\dot{\tilde{x}}_m + k_2\tilde{x}_m = 0 \quad (32)$$

The values of k_1 and k_2 can properly be selected using the standard linear control theory. Then by using the control laws of (31) the IMs can be made to follow the desired accelerations, velocities and positions.

5 Simulation, experiments and analysis

This section presents the simulation and experimental results and provides analysis.

5.1 Simulation setup and results

5.1.1 Simulation setup

Simulation is performed in the Simulink environment, and the data in Table 1 is used. The data is taken from the prototype implemented in Sect. 5.2. For simulation and experimentation T = 1 s is used. The Ode45 (Dormand–Prince) solver is used with a variable step. The maximum step size is 1 ms and the minimum step size is 0.0001 ms and the initial step size is 1 ms.
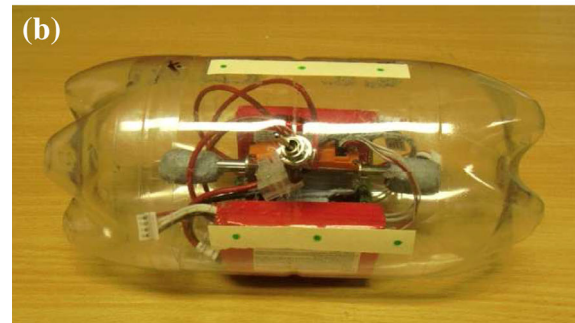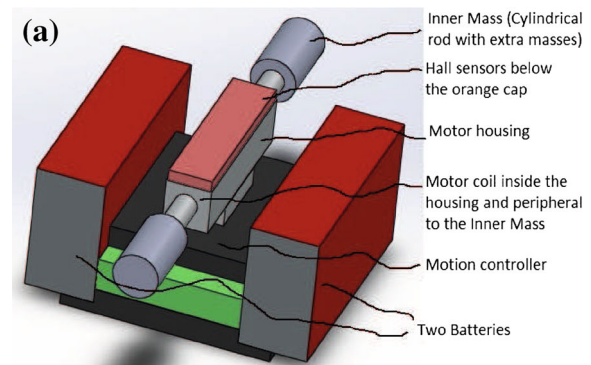
5.1.2 Simulation results

In applications the capsubot needs to follow a certain given position trajectory. In simulation the proposed algorithm is used to track the desired trajectory. The desired and simulated trajectories of the capsubot are shown in Fig. 8a. Figure 8b shows the position trajectory tracking error in simulation. Figure 8c shows the simulated IM acceleration. The required acceleration profile parameters is selected and modified/changed in each piece to make the capsubot follow the desired trajectory. Here we see for the first 8 s the IM follows the utroque acceleration profile described in Fig. 3a as the desired capsubot velocity is +ve. Then the desired capsubot velocity changes to −ve. Thus the IM follows the contrarium acceleration profile as shown in Fig. 3d for 1 cycle. Finally the IM follows the utroque acceleration profile as shown in Fig. 3b for the rest of the time.

In Fig. 8a we see that the capsubot moves comparatively faster at the beginning of the trajectory and at the last portion

(a)

(b)

(c)
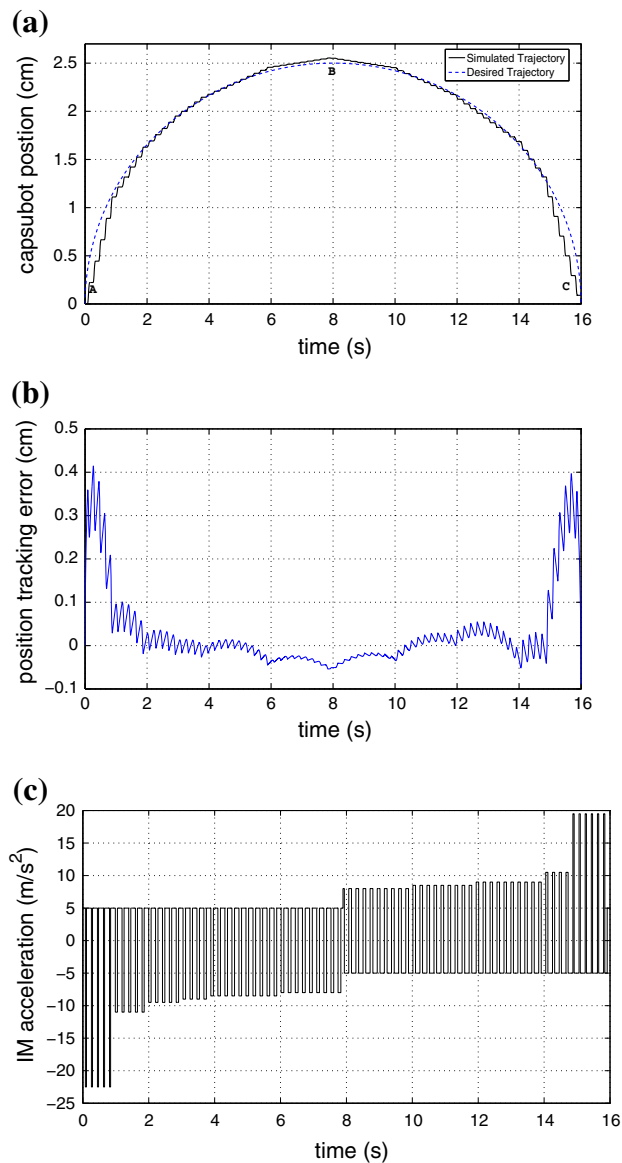
Fig. 8 Simulated results for capsubot position trajectory tracking. **a** Simulated and desired capsubot position trajectory. **b** Capsubot position trajectory tracking error in simulation. **c** Simulated IM acceleration

(a)

Inner Mass (Cylindrical rod with extra masses)

Hall sensors below the orange cap

Motor housing

Motor coil inside the housing and peripheral to the Inner Mass

Motion controller

Two Batteries

(b)

(c)

Fig. 9 CAD Design and Implemented Capsubot. **a** 3D CAD design of the Capsubot (without Capsubot-shell). **b** Implemented Capsubot: With Capsubot-shell. **c** Implemented Capsubot: Without Capsubot-shell

of the trajectory. Thus from Fig. 8c we see the IM has bigger accelerations at those times compare to times in the middle. Again at the middle part of the trajectory the capsubot moves very slowly. Thus the IM has lower accelerations at that time. From Fig. 8b we see that the position tracking error is comparatively higher at the first and last part of the trajectory i.e. the error is higher when the capsubot moves faster. Again the error is moderate in the middle part of the trajectory when the capsubot moves very slowly. In the rest of the trajectory when the capsubot moves with a moderate speed, the error is nearly zero. Thus the error increases if the required speed is too high or too low.

5.2 Experimental setup and results

5.2.1 Experimental setup and physical constraints

The 3D CAD design of the Capsubot (without Capsubot-shell) is shown in Fig. 9a. A prototype shown in Fig. 9b, c is developed based on the design and the proposed control approach is implemented for position trajectory tracking. In the experimentation, T = 1 s is used. The main components of the developed capsubot system are a linear DC motor (QUICKSHAFT LM1247-020-01), a motion controller (Minimotor 2013), two batteries and a capsubot-shell to hold all the components. The linear motor is comprised of a motor-housing which houses the coil, three hall sensors and a cylindrical rod which is capable of moving back and forth within the capsubot. The motion controller powers the

linear motor and controls the movement of the cylindrical rod by controlling the current flow to the motor coil. The coil is placed inside the motor housing and peripheral to the cylindrical rod. The motion controller is powered by two batteries. It is programmed using the Motion Manager Software (Minimotor 2013) and then can be disconnected from the PC. The capsubot is 20 cm in length and 8 cm in diameter. The cylindrical rod works as the Inner Mass (IM) of the capsubot.

It is noted that the IM includes the cylindrical rod and two extra masses at both ends of the cylindrical rod. The extra masses are added to increase IM to capsubot mass ratio. The parameters of the capsubot are listed in Table 1. The Hall sensors are used to determine the position of the cylindrical rod (IM). The linear motor data (i.e. IM position and velocity, current through the coil etc.) can be logged using the Motion Manager Software. To obtain the data for capsubot movements we recorded the motion of the capsubot using a video camera and then a video analysis software Quintic Biomechanics (Biomechanics 2013) was used to determine the position, velocity and acceleration.

The capsubot has the following physical constraints:

– The stroke length of the IM is 20 mm (Minimotor 2013) (Fig. 9a, c). In the experimentation and simulation stroke length of 18 mm ($-k \leq x_m - x_M \leq k$ where k = 9 mm) was used to avoid the collision. This constraint was considered while designing the profile parameters t_{c1}, t_{c2}, t_{u1}, t_{u2}, t_{u3} and t_{u4} of Fig. 3.
– The linear motor allows that the maximum continuous acceleration of the IM is ± 30 ms^{-2}. This limit was considered while designing the profile parameters a_{mu2}, a_{mu3} and a_{mc1} of Fig. 3.
– The maximum static friction force of the capsubot is $\mu_M M g$. This constraint was considered while designing the profile parameters a_{mu1}, a_{mu4} and a_{mc2} of Fig. 3a, c.
– Other constraints of the linear motor (LM 1247-0201-01) from the data sheet (Minimotor 2013):

    – Maximum Continuous force on the IM : 3.09 N;
    – Peak force on the IM : 9.26 N;
    – Maximum Continuous current through the motor coil: 0.48 A;
    – Peak current through the motor coil : 1.44 A;

The above mentioned constraints are met when we use acceleration within the limit ± 30 ms^{-2}.

5.2.2 Experimental results

The experimental position of the IM for capsubot position trajectory tracking is shown in Fig. 10a. The IM remains within the limit i.e. [−k, k] where k is 9 mm. Experimental position trajectory of the capsubot is shown in Fig. 10b. From the figure we see that the capsubot trajectory is not smooth
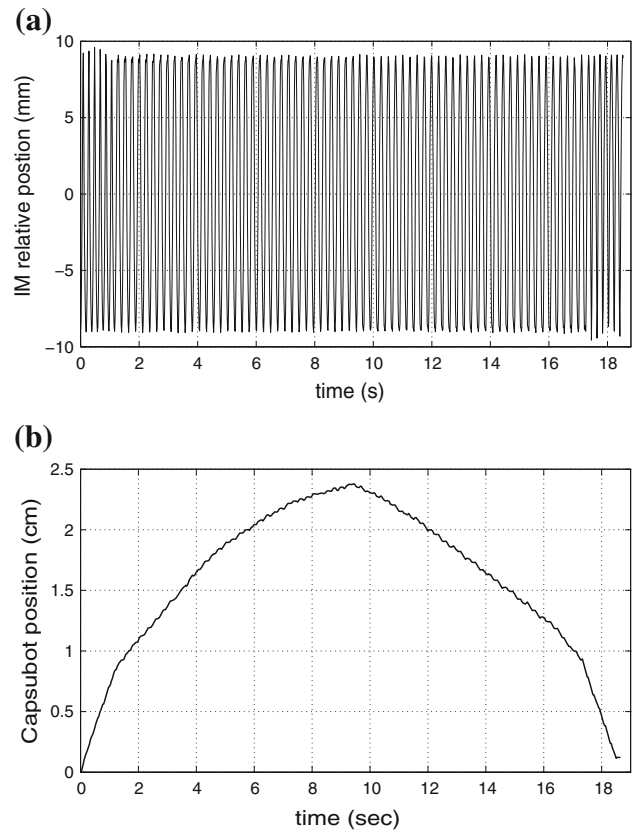
Fig. 10 Experimental results for position trajectory tracking using proposed control approach. **a** Experimental IM relative position ($x_m - x_M$). **b** Experimental capsubot position (x_M)

rather we see it going step by step. The reason behind this is the very nature of the capsubot movement principle where capsubot moves part of each cycle and remains stationary for the remaining time of the cycle.

5.3 Analysis

5.3.1 Comparison analysis

Experimental and simulation positions of the IM for 1s for position trajectory tracking are shown in Fig. 11a. Experimental, simulation and desired (target) position trajectories of the capsubot are shown in Fig. 11b.

In Fig. 11a the simulation and experimental results have the same pattern. However there are differences between the curves. The experimental result is delayed compare to the simulation result. In 11 we see that in total the capsubot experienced 2.5 s delay in the experiments than the desired and simulation results. We see that the experimental capsubot trajectory has similar pattern as the desired and simulation trajectories.

One possible reason which leads to this difference is that we only consider the capsubot dynamics and ignore the

Fig. 11 Experimental and simulation results for position trajectory tracking using proposed control approach. **a** Experimental and simulation IM position ($x_m - x_M$) for position trajectory tracking for 1 s **b** experimental and simulation capsubot position (x_M) for position trajectory tracking
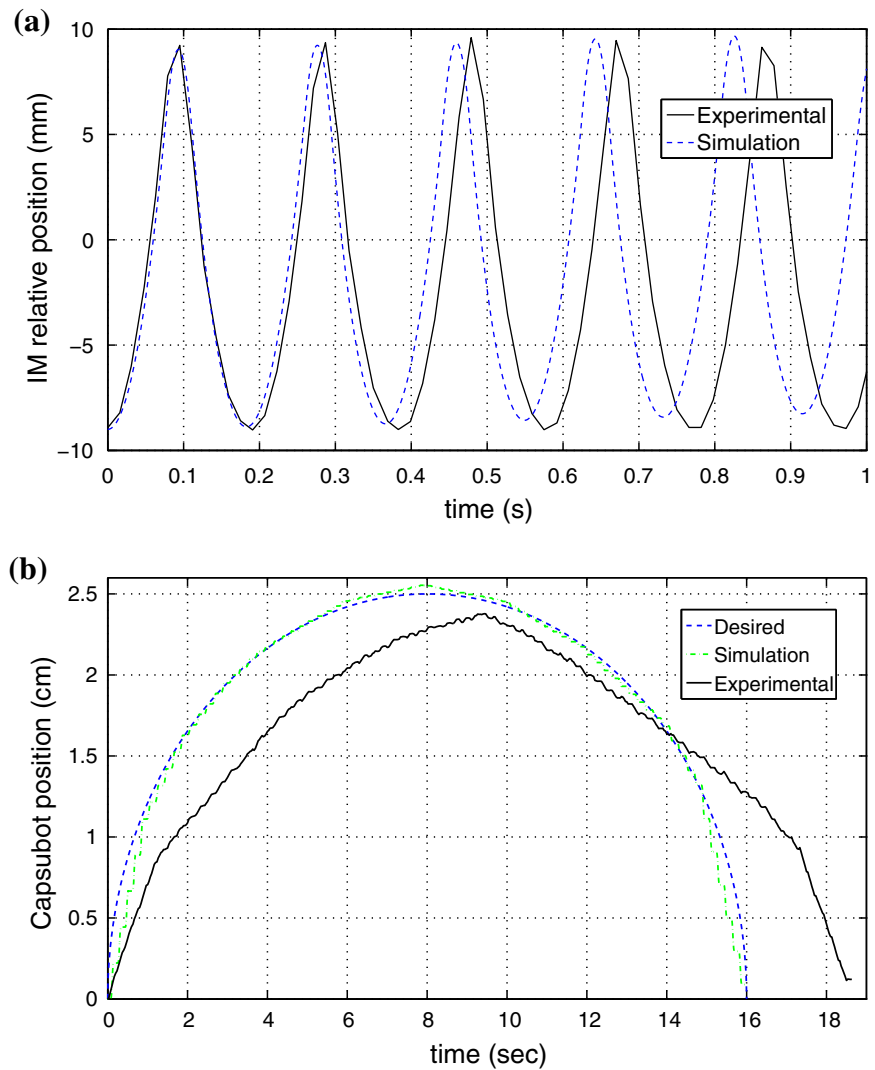
dynamics of the linear motor. Actually, the IM is actuated by energising the coil placed inside the motor housing and peripheral to the IM. The terminal inductance (phase-phase) of the coil is $820\,\mu$H. The current provided to the coil cannot be changed abruptly because of the dynamics of the linear motor. Thus the force applied to the IM and subsequently the acceleration of the IM cannot be changed abruptly. This makes the developed capsubot response in the experiment slower than that in the simulation and subsequently we get a delay in the trajectory following. However, the experimental results have demonstrated the proposed method.

Figure 12 shows the position trajectory tracking error in simulation and experimentation. Table 2 presents the maximum absolute tracking error, mean absolute error and relative mean absolute error of trajectory tracking. Simulation position trajectory tracking error is small whereas experimental position trajectory tracking error is big. One main reason of this big error is the delay in the experiments which is explained above. The other factors which might contribute
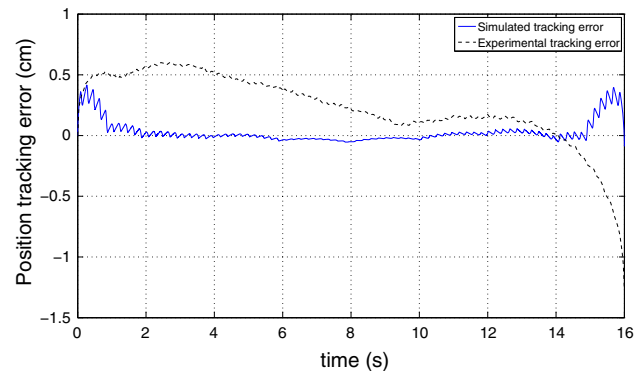
Fig. 12 Experimental and simulation capsubot position trajectory tracking error using proposed control approach

to the error are measurement noise, friction uncertainty (we used simple coulomb friction model) and other disturbances.

In our future research we will incorporate the actuator dynamics into the model and use sophisticated friction

Table 2 Comparison of the algorithm performance for simulation and experiments

Position trajectory tracking	Maximum absolute error (cm)	Mean absolute error (cm)	Relative mean absolute error* (%)
Simulation	0.41429	0.05132	2.6157
Experimentation	1.27547	0.31457	16.056

* Relative mean absolute error = (mean absolute error/mean absolute desired value)100 %

model. Other areas of improvements are to choose the piece time optimally and incorporate capsubot position feedback into the control loop.

5.3.2 Capsubot demonstration

A video is attached with the paper where the demonstration of position trajectory tracking is shown accompanied by a capsubot position (desired, simulation and experimental) versus time plot.

In the video demonstration we see that the capsubot shakes while moving. To have a smooth movement, the capsubot centre of mass should stay on the IM axis of movement. It ensures that no torque is applied on the robot. For the implemented prototype of this paper, the centre of mass doesnt reside on the axis of movement of the IM as we used off-the-shelf linear motor and controller from Faulhaber. Rather the centre of mass resides below the axis of movement of the IM. Thus the IM movement produces a torque which tries to roll over the capsubot. The torque is not big enough to roll over the capsubot. However these repetitive attempts are responsible for the shaking of the capsubot. It is possible to make purpose built capsubot where the centre of mass resides on the axis of movement of the IM as done in Lee et al. (2008). The shaking should not be a problem in that case.

The robot structure also might have contributed to the shaking of the capsubot. Here the cylindrical structure robot is moving on a flat surface. If we try the robot in cylindrical structure e.g. in pipe the shaking might reduce. On the other hand if we make the outer cover of the robot a parallelepiped and try it on flat surface the shaking might decrease.

If the capsubot can avoid shaking by using appropriate outer structure and purpose built actuator, the images taken by the robot should be without significant noise. To do a better observation i.e. to take better images of some suspected region, the robot can stop and observe/take images of the region and then move forward. It will ensure that the images are of best quality.

5.3.3 Scalability of the capsubot

The dimension of commercially available smallest linear motor is: diameter 8 mm and length 58 mm whereas the diameter and length of the cylindrical rod (which works as IM) are 4 and 58 mm respectively. The robot used in Lee et al. (2008)

is custom-built and the dimension is: diameter 7 mm and length 40 mm which gives us confidence that the capsubot can be miniaturized to be integrated with capsule endoscope. The size of a commercially available capsule endoscope is 11 mm diameter and 26 mm in length (Olympus 2014). In our future research we aim to develop custom-built capsule robot.

In Yu et al. (2011) the parameter of Lee et al. (2008) is used and the proposed four-step acceleration profile is utilized. The maximum average velocity achieved is 0.074 m/s. The maximum average velocity achieved in experiment in Lee et al. (2008) is 0.05 m/s. These results show promises of capsubot-type robot in capsule endoscopy.

6 Conclusions and future works

The paper has shown a direction for the trajectory tracking of under-actuated mechanical systems. Though trajectory tracking is one of the primary purposes of developing these types of robots, no research is done to date addressing trajectory tracking of a capsubot-type robot. We have proposed a two-stage control strategy for the motion control of an under-actuated capsubot. We have implemented the control strategy on a developed prototype. Simulation and experimental results have validated the control approach.

Two modified acceleration profiles (utroque and contrarium) have been proposed which removes the limitations of the previously proposed acceleration profiles in Yu et al. (2011). Profile parameters for the newly proposed acceleration profiles have been optimally selected considering the physical constraints. The acceleration profiles have been implemented in the developed 1D capsubot. Thus the profiles have been validated through theoretical analysis, simulation and experimentation. A novel selection algorithm for the stage 1 of the control strategy has been proposed to select the right acceleration profile (i.e. utroque or contrarium) and also to select the optimal acceleration profile parameters (acceleration values) considering the desired trajectory requirements.

The developed capsubot prototype can follow position trajectory. It is noted that there are differences between the simulation and experimental results. The future works have the following four aspects (1) investigate the impact of the actuator dynamics and other disturbances; (2) incorporate sophisticated friction model to the capsubot model (3) opti-

mally select and tune the piece time T; (4) feedback should be taken from the capsubot position and the control input should be corrected according to the error ($\dot{x}_{Me}$) value for tracking the position of the capsubot more accurately:

$$x_{Me}(i) = x_{Md}(i) - x_{Mm}(i) \tag{33}$$

x_{Me} should be utilized to modify $\bar{\dot{x}}_{Md}$ at the start of each piece. Equation (16) is modified as follows:

$$\bar{\dot{x}}_{Md}(i) = \frac{\delta x_M(i) + x_{Me}(i-1)}{T} \tag{34}$$

References

Aguiar, A. P., & Hespanha, J. P. (2007). Trajectory-tracking and path-following of underactuated autonomous vehicles with parametric modeling uncertainty. *IEEE Transactions on Automatic Control*, *52*(8), 1362–1379.

Ashrafiuon, H., Muske, K. R., McNinch, L. C., & Soltan, R. A. (2008). Sliding-mode tracking control of surface vessels. *IEEE Transactions on Industrial Electronics*, *55*(11), 4004–4012.

Bi, F., Wei, Y., Zhang, J., & Cao, W. (2010). Position-tracking control of underactuated autonomous underwater vehicles in the presence of unknown ocean currents. *IET Control Theory & Applications*, *4*(11), 2369–2380.

Biomechanics Q (2013). Retrieved 12 December 2013, from http://www.quintic.com/.

Carpi, F., Kastelein, N., Talcott, M., & Pappone, C. (2011). Magnetically controllable gastrointestinal steering of video capsules. *IEEE Transactions on Biomedical Engineering*, *58*(2), 231–234.

Carta, R., Sfakiotakis, M., Pateromichelakis, N., Thoné, J., Tsakiris, D., & Puers, R. (2011). A multi-coil inductive powering system for an endoscopic capsule with vibratory actuation. *Sensors and Actuators A: Physical*, *172*(1), 253–258.

Chernous'ko, F. (2002). The optimum rectilinear motion of a two-mass system. *Journal of Applied Mathematics and Mechanics*, *66*(1), 1–7.

Do, K. D., Jiang, Z. P., & Pan, J. (2003). On global tracking control of a vtol aircraft without velocity measurements. *IEEE Transactions on Automatic Control*, *48*(12), 2212–2217.

Huang, J., Ding, F., Fukuda, T., & Matsuno, T. (2013). Modeling and velocity control for a novel narrow vehicle based on mobile wheeled inverted pendulum. *IEEE Transactions on Control Systems Technology*, *21*(5), 1607–1617.

Lee, N., Kamamichi, N., Li, H., & Furuta, K. (2008). Control system design and experimental verification of capsubot. In: *Proceedings of the IEEE/RSJ International Conference on Intelligent Robots and Systems* (pp. 1927–1932). IEEE

Liu, Y., Yu, H., & Yang, T. (2008). Analysis and control of a capsubot. In: *Proceedings of the 17th World Congress the International Federation of Automatic Control* (pp. 756–761).

Lopez-Martinez, M., Acosta, J., & Cano, J. (2010). Non-linear sliding mode surfaces for a class of underactuated mechanical systems. *IET Control Theory & Applications*, *4*(10), 2195–2204.

Menciassi, A., Accoto, D., Gorini, S., & Dario, P. (2006). Development of a biomimetic miniature robotic crawler. *Autonomous Robots*, *21*(2), 155–163.

MINIMOTOR SA S (2013) Retrieved 12 December, 2013 from http://www.faulhaber-group.com/.

Olympus (2014) Endocapsule system. Retrieved August, 2014, from http://www.olympus.co.uk/

Park, M. S., & Chwa, D. (2009). Swing-up and stabilization control of inverted-pendulum systems via coupled sliding-mode control method. *IEEE Transactions on Industrial Electronics*, *56*(9), 3541–3555.

Pathak, K., Franch, J., & Agrawal, S. (2005). Velocity and position control of a wheeled inverted pendulum by partial feedback linearization. *IEEE Transactions on Robotics*, *21*(3), 505–513.

Valdastri, P., Webster, R., Quaglia, C., Quirini, M., Menciassi, A., & Dario, P. (2009). A new mechanism for mesoscale legged locomotion in compliant tubular environments. *IEEE Transactions on Robotics*, *25*(5), 1047–1057.

Xu, R., & Özgüner, Ü. (2008). Sliding mode control of a class of underactuated systems. *Automatica*, *44*(1), 233–241.

Yamagata, Y., & Higuchi, T. (1995). A micropositioning device for precision automatic assembly using impact force of piezoelectric elements. In: *Proceedings of the 1995 IEEE International Conference on Robotics and Automation* (vol. 1, pp. 666–671). IEEE

Yu, H., Liu, Y., & Yang, T. (2008). Closed-loop tracking control of a pendulum-driven cart-pole underactuated system. *Proceedings of the Institution of Mechanical Engineers, Part I: Journal of Systems and Control Engineering*, *222*(2), 109–125.

Yu, H., Huda, M., & Wane, S. (2011). A novel acceleration profile for the motion control of capsubots. In: *Proceedings of the 2011 IEEE International Conference on Robotics and Automation* (pp. 2437–2442). IEEE

Zhang, Y., Jiang, S., Zhang, X., Ruan, X., & Guo, D. (2011). A variable-diameter capsule robot based on multiple wedge effects. *IEEE/ASME Transactions on Mechatronics*, *16*(2), 241–254.
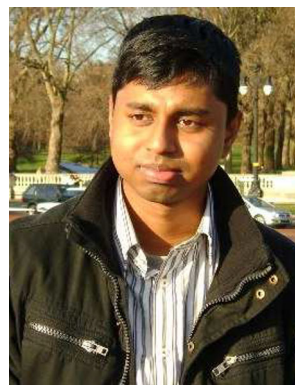
M. Nazmul Huda received his BSc in Electrical and Electronic Engineering from Bangladesh University of Engineering and Technology, Bangladesh in 2008 and MRes in Computing Science from Staffordshire University, UK in 2011. He is currently a Ph.D. student in Robotics at Bournemouth University, UK. He is also an RA in the Faculty of Engineering and Computing at Coventry University, UK. Previously he worked as a lecturer in the Department of Electrical and Electronic Engineering at Ahsanullah University of Science and Technology (AUST) in Bangladesh. His research interests include robotics for medical applications, micro and nano robotics, control systems etc.

Hongnian Yu is currently a Professor of Computer Science at Faculty of Science and Technology, Bournemouth University. His researches cover Robotics, Wireless networked control systems, RFID and its applications, mobile computing, modelling, scheduling, planning, and simulations of large discrete event dynamic systems with applications to manufacturing systems, supply chains, transportation networks and computer networks. He has published over 200 research papers. He has held several research grants worth about three million pounds from EPSRC, the Royal Society, and the EU, AWM, as well as from industry. He has successfully completed an EU funded Asia-Link project (Euro-Asia Collaborations and Networking in Information Engineering System Technology) and currently is supervising two EU projects (east-west Link for Innovation, Networking and Knowledge exchange, 5.5 million Euro) and (Sustainable E-Tourism, 2.5 million Euro). He was a General Chair of International conference on Software Knowledge Information Management and Applications (SKIMA) in 2006, and is serving on various other conferences and academic societies.